Optics Letters

Layout of NALM fiber laser with adjustable peak power of generated pulses

Sergey Smirnov,[1,*] Sergey Kobtsev,[1,2] Alexey Ivanenko,[1] Alexey Kokhanovskiy,[1] Anna Kemmer,[1] and Mikhail Gervaziev[1]

[1]Division of Laser Physics and Innovative Technologies, Novosibirsk State University, Pirogova str., 2, Novosibirsk 630090, Russia
[2]Tekhnoscan-Lab LLC, Inzhenernaia str., 26, Novosibirsk 630090, Russia
*Corresponding author: smirnov@lab.nsu.ru

Received 6 March 2017; revised 31 March 2017; accepted 1 April 2017; posted 4 April 2017 (Doc. ID 287932); published 21 April 2017

The Letter proposes a new layout of a passively mode-locked fiber laser based on a nonlinear amplifying loop mirror (NALM) with two stretches of active fiber and two independently controlled pump modules. In contrast with conventional NALM configurations using a single piece of active fiber that yields virtually constant peak power, the proposed novel laser features larger than a factor of 2 adjustment range of peak power of generated pulses. The proposed layout also provides independent adjustment of duration and peak power of generated pulses as well as power-independent control of generated pulse spectral width impossible in NALM lasers with a single piece of active fiber.

OCIS codes: (140.0140) Lasers and laser optics; (060.3510) Lasers, fiber; (140.4050) Mode-locked lasers; (140.3410) Laser resonators; (140.7090) Ultrafast lasers.

https://doi.org/10.1364/OL.42.001732

Fiber lasers mode-locked due to nonlinear optical loop mirrors (NOLM) [1,2] and nonlinear amplifying loop mirrors (NALM) [3], also known as figure-of-eight lasers, are widely used practical tools for ultra-short pulse generation. NOLM- and NALM-based lasers are robust, do not contain material-based saturable absorbers, and thus demonstrate virtually unlimited lifetime and absence of specific power limitations except thermal damage threshold of fiber optical components. The latter fact allows one to obtain relatively high output pulse energies directly in a master oscillator with no additional external optical amplifiers [4]. Taking advantage of wavelength-independent Kerr nonlinearity for mode locking allows one to operate NALM lasers in different spectral ranges using Yb-, Er-, and Tm-doped fibers as active media [5–7]. In contrast with fiber lasers based on the nonlinear polarization evolution (NPE) effect, which also benefit from absence of material-based saturable absorbers and thus can deliver relatively high pulse energies [8–10], NALM/NOLM lasers may be designed in an all-polarization-maintaining (PM) configuration, thereby further improving their stability and robustness [11]. NALM lasers are capable of producing femtosecond-scale pulses either after compensation of a large normal cavity dispersion of Yb fiber lasers [12,13] or directly in the solitonic regime in anomalous dispersion configuration [14].

Despite the fact that numerous parameters determine performance of NALM/NOLM, once the laser is assembled, reflectivity/transmittance of fiber loop mirror depends only on power of intra-cavity radiation and cannot be controlled. This makes NOLM/NALM lasers inflexible, leaving a single degree of freedom by allowing the user to vary pump power level only. Although the latter can be adjusted over a relatively wide range in some configurations, this results in energy scaling at virtually constant peak power [15–18]. In contrast, adjustment of polarization controller settings in NPE-based lasers provides access to a plethora of lasing regimes that can differ from each other not only quantitatively (in pulse energy, duration, peak power, etc.) but even qualitatively as well [19–21]. Although different lasing regimes in NALM lasers have been demonstrated up to date [4], previously reported NALM configurations with a single stretch of active fiber and a single pump module (we will refer to them hereafter as conventional NALM configurations) provide much narrower possibilities of lasing adjustment, which may be a limiting factor in some applications. This Letter shows for the first time how this NALM issue can be overcome in our novel layout using two independently pumped stretches of active fiber inside a loop mirror. Proper adjustment of each of two pump powers permits adjustment of the peak power of the generated pulses by more than a factor of 2, provides access to a large variety of lasing regimes, and also allows us to control duration and spectral width of laser pulses generated in the proposed layout, which is something impossible in conventional NALM lasers relying on a single stretch of active fiber.

The novel fiber laser setup proposed in the present work is schematically shown in Fig. 1. The laser comprises two fiber loops, namely, a passive loop and NALM, only containing PM fiber and PM components and connected via a 40/60 coupler. NALM includes two stretches of double-clad Yb fiber, YDF1 and YDF2, of length 5.3 and 5 m correspondingly, separated by 12.4 m of passive PM fiber. Active fibers are pumped through pump combiners with two independently controlled

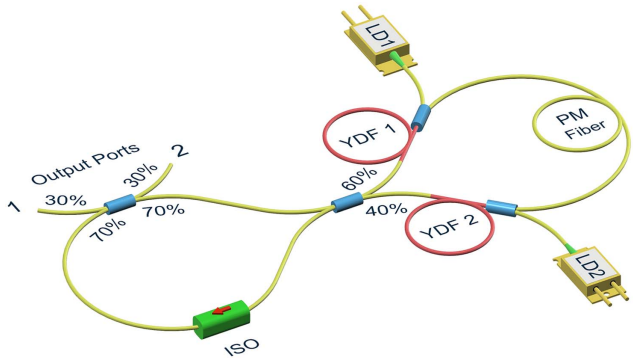

Fig. 1. Diagram of the experimental setup: LD1&2, pumping laser diodes; ISO, fiber isolator; YDF 1&2, stretches of ytterbium-doped fiber of lengths $L_1 = 5.3$ m and $L_2 = 5$ m; PM fiber, stretch of PM fiber of length $L_0 = 12.4$ m.

multi-mode laser diodes LD1 and LD2 emitting at 978 nm. The passive loop comprises an optical isolator and a 30/70 fiber optical coupler, two ports of which are used as laser exits. The length of the passive loop is 2.8 m, and the total cavity length is about 28.7 m, corresponding to pulse repetition rate of 7.26 MHz, see Fig. 2. Stable mode-locking is observed starting from 1.6 W pump power delivered to both YDF1 and YDF2 fibers each. At this pump level, the laser produces 11 nJ pulses.

In order to obtain deeper insight into lasing dynamics of the proposed laser configuration with two independently pumped stretches of active fiber, we use a numerical model based on a nonlinear Schrödinger equation [22]:

$$\pm\frac{\partial A}{\partial z} = i\gamma|A|^2A - \frac{i}{2}\beta_2\frac{\partial^2 A}{\partial t^2} + \frac{Ag_0/2}{1 + W/(P_{\text{sat}}\cdot\tau)}, \quad (1)$$

where sign $\pm$ corresponds to the forward and backward counterpropagating waves, $A(z, t)$ is the optical field envelope, z stands for the longitudinal coordinate along the fiber, t is time in the retarded frame of reference, γ and β_2 are nonlinear and dispersion coefficients correspondingly, g_0 and P_{sat} stand for unsaturated gain coefficient and saturation power for the active fiber, τ is cavity round-trip time, $W = W^+ + W^- = \int(|A^+|^2 + |A^-|^2)dt$ is the total energy of counterpropagating waves. Assuming $g_0 = 0$, we can use Eq. (1) to describe laser pulse propagation through passive fibers as well. In our simulations, we varied saturation energies $W_{\text{sat}} = \tau P_{\text{sat}}$ of both active fibers from 0.1 up to 30 nJ in order to model variation of pump powers of NALM. Numerical model (1) is widely used, allowing adequate reproduction of lasing dynamics and properties of picosecond fiber lasers (see e.g., [8,23,24]).

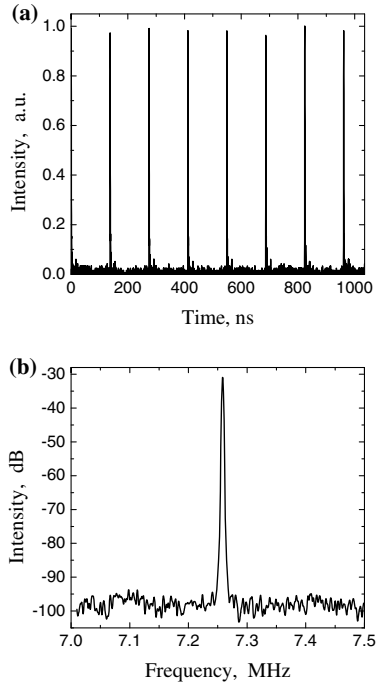

Fig. 2. (a) Generated pulse train. (b) RF spectrum.

Let's note that laser pulses travel within the NALM in both directions and that both waves saturate the active fibers. Thus, Eq. (1) is in fact a system of two coupled equations for counterpropagating waves, which is solved in two stages during each cavity round-trip simulation. In the first stage, self-consistent energy distributions $W^{\pm}(z)$ of counterpropagating waves are evaluated according to Eq. (2), which can be derived from Eq. (1):

$$\frac{dW^{\pm}}{dz} = \pm\frac{g_0 W}{1 + W/(P_{\text{sat}}\cdot\tau)}. \quad (2)$$

Once $W^+(z)$ and $W^-(z)$ are known, at the second stage we can integrate Eq. (1) independently for A^+ and A^- using the well-known split-step Fourier method [22].

A 10-ps sech^2 seed pulse is used as the initial condition for the first cavity round-trip. Numerical simulation of up to 10^4 successive cavity round-trips is performed. However, it is interrupted earlier either if the program reaches the limit cycle of the propagation equations (i.e., pulse parameters remain constant to the accuracy of no worse than 10^{-5}) or if the pulse dissipates or splits into continuous waves. As will be shown below, the numerical model allowed us to adequately reproduce experimental results obtained with our novel laser layout.

In order to better understand the merits of the proposed novel NALM configuration, let's first consider operation of a conventional NALM with a single active fiber. To do that, we will substitute the active fiber connected to the 40% coupler port (see Fig. 1) with a stretch of passive fiber of the same length. In our simulations, we vary the saturation energy of the single remaining active fiber, obtaining a range of lasing regimes in which the laser yields dissipative soliton resonance (DSR) [21,25]. DSR has a nearly rectangular temporal profile and can carry relatively high energy at high pump powers due to pulse elongation at virtually constant peak power (see Fig. 3 (a) and [15]). Peak power level persistence in NALM/NOLM lasers with a single active fiber can be readily understood from consideration of transmittance coefficient T of the nonlinear fiber loop [1]. For the sake of simplicity, let's assume the length of active fiber to be negligible in comparison with the passive fiber length $L = L_0 + L_2 = 17.4$ m inside NALM. In this approximation, we can write down the NALM reflectivity for incident laser pulse of peak power P [1]:

$$T = g\cdot[1 - 2\alpha(1-\alpha)(1+\cos\delta\varphi)]. \quad (3)$$

Here g is the amplification coefficient of the active fiber, $\alpha = 0.6$ is the coupling ratio, and $\delta\varphi$ stands for the differential phase shift of the counterpropagating waves:

$$\delta\varphi = \gamma PL(\alpha g - (1-\alpha)). \quad (4)$$

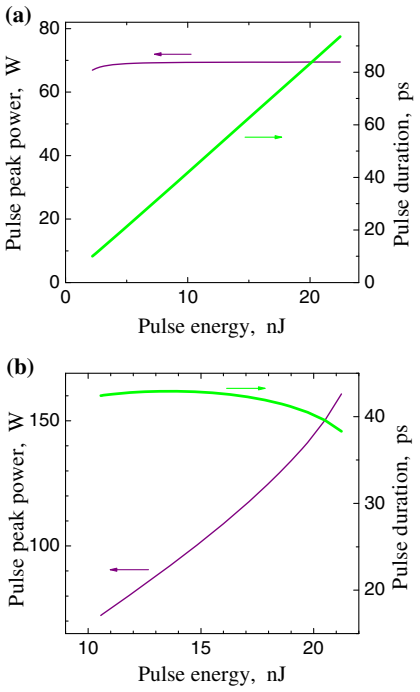

Fig. 3. Simulated dependence of the pulse peak power and rms pulse duration on pulse energy with (a) only one (first) and (b) both pumps used; the second pump (at 40% port) is varied.

Once the laser is mode-locked, it operates at maximum of transmission curve [2], which corresponds to $\delta\varphi = \pi$ and $P = \pi/[\gamma PL \cdot (\alpha g - 1 + \alpha)]$. It must be noted that gain of the active fiber g precisely compensates for optical losses during stationary pulse generation. This leads to $g \approx$ const and consequently $P \approx$ const, as corroborated by the results of numerical simulations [see Fig. 3(a)] as well as by previously reported studies both in the cases of normal [15–18] and anomalous [14,26] dispersion.

A completely different situation takes place when two independently pumped stretches of active fiber are used. In this case, the nonlinear phase shift difference of counterpropagating waves [Eq. (4)] transforms into

$$\delta\varphi = \gamma PL \cdot (\alpha g_1 - (1 - \alpha) g_2), \tag{5}$$

where g_1, g_2 stand for the amplification coefficients of two active fibers, and their product $g_1 g_2$ compensates for optical losses. Because g_1 or g_2 can be varied independently keeping $g_1 g_2 \approx$ constant, the pulse peak power $P = \pi/[\gamma L \cdot (\alpha g_1 - (1 - \alpha) g_2)]$ is no longer constant and can be varied from 70 W up to 160 W in our configuration, as illustrated in Fig. 3(b). Thus, the proposed layout enables more than a factor of 2 variation of the peak power in a stark difference from the conventional NALM configuration with a single active fiber where peak power remains virtually constant at varying levels of pump power. It also should be noted that the proposed NALM layout has two adjustable powers, P_1 and P_2. Figure 3(b) shows only one possible way of their adjustment, namely, $P_1 =$ const, which results in virtually constant pulse duration and nearly linear growth of the peak power with energy. Increasing pump powers by following different paths on the plane (P_1, P_2), one can achieve higher pulse energy either due to an increase in the peak power, due to pulse elongation, or due to a combination of both in different proportions. Thus, the proposed novel layout opens access to a large variety of lasing regimes and paves the way for easily reliable and reproducible live electronic adjustment of lasing properties.

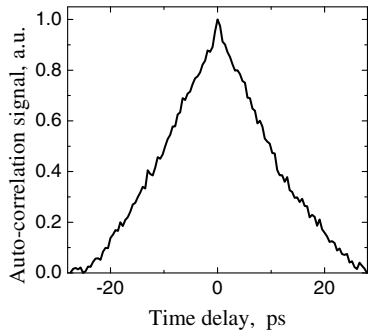

Fig. 4. Central fragment of the measured triangular auto-correlation function agrees well with the Π-shaped simulated DSR.

Because the laser under consideration generated relatively long pulses (DSR with rms-width of dozens of picoseconds [see Fig. 3]), we were unable to measure pulse duration directly using our autocorrelator with a dynamic range of 33 ps. A typical measured central fragment of the auto-correlation function (ACF) rescaled to interval from 0 to 1 is shown in Fig. 4. A nearly triangular shape of ACF corresponds to a Π-shaped DSR obtained in numerical simulations. A slightly distorted ACF shape may come as a result of the input beam being partially blocked at the edges of the autocorrelator scanning range. Being unable to measure the pulse width and therefore evaluate the pulse peak power experimentally, we compare the simulated and measured spectral width at different levels of pulse energies.

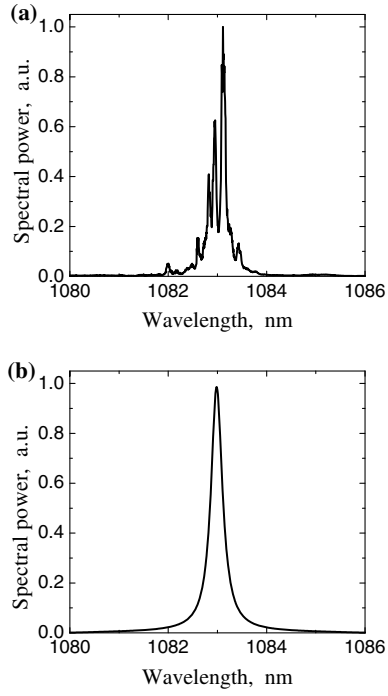

Fig. 5. Typical example of (a) measured and (b) simulated optical spectra.

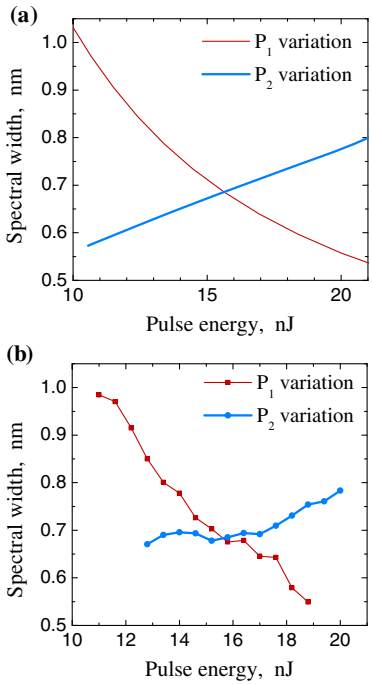

Fig. 6. Spectral width (rms) as a function of generated pulse energy under variation of the first and second pump sources. (a) Experimental results. (b) Numerical simulation.

In order to measure the output optical spectrum, we connected an optical spectrum analyzer with resolution of 0.02 nm (Yokogawa AQ6370) to output port 2, see Fig. 1. Output port 1 delivered similar but slightly wider spectra. However, due to excessive noise level intrinsic to port 1, we used main port 2 for all measurements. Typical shapes of measured and simulated optical spectra at the output port 2 are shown in Figs. 5(a) and 5(b), respectively.

When pump power P_1 at the 60% coupler port is increased, the spectral width of generated pulses is reduced by almost half both in experiment and simulations (see red line in Fig. 6). Good qualitative agreement between the simulated and measured curves in Fig. 6 suggests that the employed numerical model is valid. Let's also note that variation of pump power P_1 only is analogous to the conventional NALM configuration where only one pump LD1 is used. Similar reduction of spectral width with pump power growth takes place in the conventional NALM configuration along with temporal lengthening of DSR. Qualitatively different spectral width dynamics is observed when the other pump power (P_2) is increased while $P_1 = \text{const}$ (see blue lines in Fig. 6). In this case, spectral bandwidth of generated pulses exhibits moderate growth as opposed to reduction in the conventional NALM configurations with a single active fiber. Despite the fact that the spectral bandwidth growth is slightly more pronounced in simulations, experimental and measured curves are also in good qualitative agreement, thus corroborating the results of numerical simulations and conclusions based on them.

In conclusion, we demonstrated for the first time a novel layout of a NALM laser with a second active fiber and a corresponding pump source module. The proposed novel layout enables more than a factor of 2 variation of the peak power of generated pulses, a result not achievable in conventional NALM layouts with a single active fiber, where the generated peak power remains virtually independent of the pump power level. The proposed configuration combines reliability and robustness of the conventional NALM with flexibility of NPE lasers providing access to a large variety of lasing regimes with adjustable power-independent pulse duration and spectral width. Moreover, the proposed NALM layout permits reliable and reproducible live electronic adjustment of lasing regimes, which is practically impossible to do by adjusting fiber-based polarization controllers in NPE lasers [23,24].

Funding. Ministry of Education and Science of the Russian Federation (Minobrnauka) (14.B25.31.0003, 3.5572.2017/BCH, 3.889.2017/PCH); Russian Foundation for Basic Research (RFBR) (16-02-00104, 16-32-60160); Foundation for Promotion of Small Enterprises in Science and Technology (138AGR/18581).

REFERENCES

1. N. Doran and D. Wood, Opt. Lett. **13**, 56 (1988).
2. I. Duling, C. Chen, P. Wai, and C. Menyuk, IEEE J. Quantum Electron. **30**, 194 (1994).
3. M. E. Fermann, F. Haberl, M. Hofer, and H. Hochreiter, Opt. Lett. **15**, 752 (1990).
4. Y. S. Fedotov, A. V. Ivanenko, S. M. Kobtsev, and S. V. Smirnov, Opt. Express **22**, 31379 (2014).
5. N. Kuse, J. Jiang, C.-C. Lee, T. Schibli, and M. Fermann, Opt. Express **24**, 3095 (2016).
6. J. Nicholson and M. Andrejco, Opt. Express **14**, 8160 (2006).
7. M. A. Chernysheva, A. A. Krylov, P. G. Kryukov, and E. M. Dianov, IEEE Photon. Technol. Lett. **24**, 1254 (2012).
8. S. Smirnov, S. Turitsyn, S. Kobtsev, and S. Kukarin, *Mode-Locked Fibre Lasers with High-Energy Pulses* (Intech, 2011).
9. J. Zhou and X. Gu, in *Conference on Lasers and Electro-Optics (CLEO)* (Optical Society of America, 2015), paper SM3P.1.
10. B.-K. Yang, S.-P. Chen, H. Chen, X. Qi, and J. Hou, Appl. Opt. **55**, 8126 (2016).
11. M. E. Fermann and I. Hartl, Nat. Photonics **7**, 868 (2013).
12. A. Avdokhin, S. V. Popov, and J. Taylor, Opt. Express **11**, 265 (2003).
13. J. Nicholson, S. Ramachandran, and S. Ghalmi, Opt. Express **15**, 6623 (2007).
14. I. N. Duling, Electron. Lett. **27**, 544 (1991).
15. J.-H. Yang, C.-Y. Guo, S.-C. Ruan, D.-Q. Ouyang, H.-Q. Lin, Y.-M. Wu, and R.-H. Wen, IEEE Photon. J. **5**, 1500806 (2013).
16. S.-K. Wang, Q.-Y. Ning, A.-P. Luo, Z.-B. Lin, Z.-C. Luo, and W.-C. Xu, Opt. Express **21**, 2402 (2013).
17. H. Lin, C. Guo, S. Ruan, and J. Yang, Laser Phys. Lett. **11**, 085102 (2014).
18. X. H. Li, Y. S. Wang, W. Zhao, W. Zhang, Z. Yang, X. H. Hu, H. S. Wang, X. L. Wang, Y. N. Zhang, Y. K. Gong, C. Li, and D. Y. Shen, Laser Phys. **21**, 940 (2011).
19. P. Grelu and N. Akhmediev, Nat. Photonics **6**, 84 (2012).
20. D. Churkin, S. Sugavanam, N. Tarasov, S. Khorev, S. V. Smirnov, S. M. Kobtsev, and S. K. Turitsyn, Nat. Commun. **6**, 7004 (2015).
21. N. Akhmediev, J. M. Soto-Crespo, and P. Grelu, Phys. Lett. A **372**, 3124 (2008).
22. G. P. Agrawal, *Nonlinear Fiber Optics* (Academic, 2007).
23. S. Kobtsev, S. Kukarin, S. Smirnov, S. Turitsyn, and A. Latkin, Opt. Express **17**, 20707 (2009).
24. S. Kobtsev, S. Smirnov, S. Kukarin, and S. Turitsyn, Opt. Fiber Technol. **20**, 615 (2014).
25. P. Grelu, W. Chang, A. Ankiewicz, J. M. Soto-Crespo, and N. Akhmediev, J. Opt. Soc. Am. B **27**, 2336 (2010).
26. K. Krzempek, Opt. Express **23**, 30651 (2015).